Wagner Da Rocha, Carlile Lavor, Leo Liberti, Thérèse Malliavin, Pseudo-dihedral angles in proteins providing a new description of the Ramachandran map, in F. Nielsen and F. Barbaresco (eds.), Geometric Science of Information (GSI), LNCS 14072:511-519, Springer, Berlin, 2023

Pseudo-dihedral angles in proteins providing a new description of the Ramachandran map*

Wagner Da Rocha[1,2][0000−0002−3894−4002], Carlile Lavor[3][0000−0002−8105−3627], Leo Liberti[2][0000−0003−3139−6821], and Thérèse E Malliavin[1][0000−0002−3276−3366]

[1] Laboratoire de Physique et Chimie Théorique, CNRS UMR7019 et Université de Lorraine, France therese.malliavin@univ-lorraine.fr
[2] Laboratoire d'Informatique de l'Ecole Polytechnique, CNRS UMR 7161, France leo.liberti@polytechnique.edu, wagner.rocha@lix.polytechnique.fr
[3] University of Campinas (IMECC - UNICAMP), Brazil clavor@unicamp.br

Abstract. Since the first years of structural biology, the Ramachandran map has provided a simple definition of the curvilinear geometry of the protein backbone. This definition is mainly based on the values of the dihedral angles ϕ and ψ measured between the heavy atoms of the protein backbone. Nevertheless, angle value discontinuities are observed, particularly in the region of the β-strand secondary structure. We introduce new pseudo-dihedral angles involving hydrogen positions instead of some of the positions of the heavy atoms. We determine simple numerical relationships between the old and new dihedral angles. We show that combining the old and new parameters allows us to overcome the discontinuity problem encountered in the Ramachandran map.

Keywords: interval Branch-and-Prune · pseudo-dihedral angles · Ramachandran map.

1 Introduction

The flourishing development of structural biology has been conducted to the availability of numerous protein structures. These structures can be considered as geometrical objects provided by nature and are therefore the subject of ongoing interest [5,9,13]. A reasonable quantification of the geometry in proteins is essential for a better definition of the biological function and activity of these molecules. The approaches easing this quantification are thus crucial for application-oriented developments in health and biotechnology.

For a decade, the development of the Branch-and-Prune (BP) and interval Branch-and-Prune (iBP) algorithms has provided a theoretical framework for the parametrization as well as a systematic enumeration of the atomic coordinates [4]. Nevertheless, the practical application of these algorithms to ever larger proteins requires further development. In this paper, we present a geometric relationship between the protein backbone dihedral angles ϕ and ψ to

* Supported by CNPq, FAPESP, UNICAMP, CNRS, Ecole Polytechnique and Université de Lorraine.

pseudo-dihedral angles defined from backbone atoms, including hydrogens. Furthermore, we calibrate these formulas experimentally on data from sets of protein structures. This new way to observe the curvilinear geometry of the backbone angles allows us to solve a discontinuity problem present in the classical definition of the Ramachandran map [10]. Removing the discontinuity helps to improve the systematic enumeration of protein conformations in the iBP algorithm [6] by avoiding the definition of multiple intervals due to the gaps in angle values.

2 Theory

The dihedral angles in protein structures are defined for sets of four atoms $A,\ B,\ C$ and D as the angles between the vectors normal to the planes $\{A, B, C\}$ and $\{B, C, D\}$. Considering two amino acid residues in a protein, consecutive in the primary sequence, R_i and R_{i+1}, the backbone dihedral angles are defined as [8]:

$$\phi_i := C^{i-1} - N^i - C^i_\alpha - C^i,\ \psi_i := N^i - C^i_\alpha - C^i - N^{i+1}, \tag{1}$$

and $\omega_i := C^{i-1}_\alpha - C^{i-1} - N^i - C^i_\alpha$, where the ω_i angle populates two sets of values: $\omega_i \approx 0^\circ$, in the case of the *cis* peptide bond, or $|\omega| \approx 180^\circ$ in the case of the *trans* peptide bond.

By analogy with the definition from (1), and considering the amino acids residues $R_j,\ R_i$, and R_{i+1}, we define the following pseudo-dihedral angles:

$$\begin{aligned}
\nu^\kappa_{ji} &:= C^{i-1} - N^i - C^i_\alpha - H^j_\kappa, & \upsilon^\kappa_{ji} &:= N^i - C^i_\alpha - C^i - H^j_\kappa,\\
\xi^\rho_i &:= H^i_\rho - N^i - C^i_\alpha - C^i, & \zeta^\varrho_i, &:= H^{i+1}_\varrho - C^i_\alpha - C^i - N^{i+1},\\
\mu^{\kappa\rho}_{ji} &:= H^j_\kappa - N^i - C^i_\alpha - H^i_\rho, & \eta^{\kappa\varrho}_{ji} &:= H^j_\kappa - C^i_\alpha - C^i - H^{i+1}_\varrho,
\end{aligned} \tag{2}$$

where $\rho \in \{\alpha,\ \alpha_2\},\ \varrho \in \{N,\ \delta_3\}$, and κ represents any character that names a hydrogen atom in a protein. Two particular cases have to be considered: in Glycine residues, two hydrogen atoms are bonded to the C_α atom, H_{α_2} and H_{α_3} [8], and we select H_{α_2} to play the role of H_α; in Proline residues, no H_N atom is present, and we choose the H_{δ_3} atom to play the role of H_N.

As the backbone angles are defined in the interval $(-180^\circ, 180^\circ]$, all pseudo-dihedral angles expressed in this paper are also in this interval, and obey the same orientation: the counter-clockwise sense is positive and clockwise sense is negative. Concerning equations (1) and (2), the angles $\nu^\kappa_{ji},\ \xi^\rho_i$, and $\mu^{\kappa\rho}_{ji}$ are associated to the angle ϕ_i and the others to the angle ψ_i. We note that all angle definitions share the same two central atoms.

We present some examples about pseudo-dihedral angles in a protein structure. If R_i is neither a Proline nor a Glycine amino acid residue, assuming $i = j$, then $\kappa = N$ and $\rho = \alpha$ in the pseudo-dihedral angles defined in (2). To simplify the notation in this case, we consider $\nu_i \equiv \nu^N_{ii},\ \xi_i \equiv \xi^\alpha_i$, and $\mu_i \equiv \mu^{N\alpha}_{ii}$. In Fig. 1, the case where $|\nu_i| \approx 180^\circ$ and $\xi_i \approx -120^\circ$ is presented.

The dihedral angles are represented in 2D in Fig. 1 (d) to (f) without loss of generality, because we can always define an isometric function to switch the

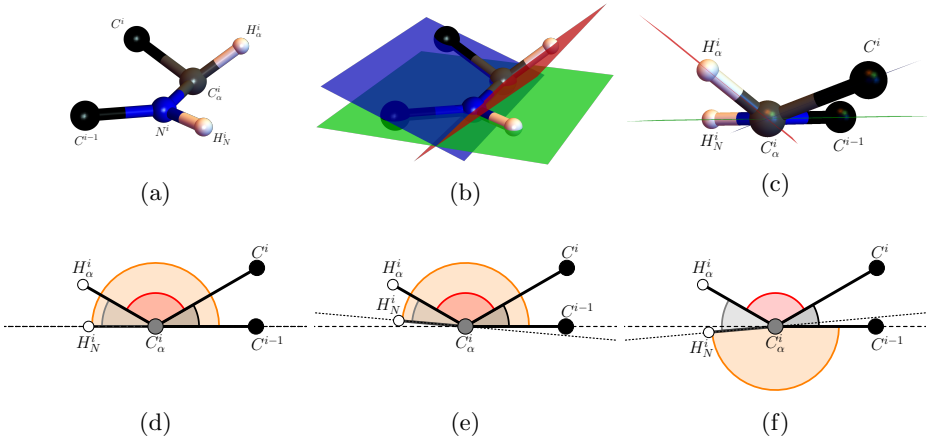

Fig. 1. (a) Spatial positions for the atoms C^{i-1}, N^i, H^i_N, C^i_α, H^i_α, and C^i whether $\nu_i = 180°$, $\xi_i = -120°$, and $\phi_i = 30°$. The numerical values bond length and bond angles are taken from [1]; (b) Definition of the planes $\{C^{i-1}, N^i, C^i_\alpha\}$ (green), $\{N^i, C^i_\alpha, C^i\}$ (blue), and $\{N^i, C^i_\alpha, H^i_\alpha\}$ (red) on the image (a) structure; (c) Rotation of image (b) structure identifying a pertinent point of view; (d) Orthogonal projection of the image (c) structure to the plane perpendicular to the bond $N^i - C^i_\alpha$. The dihedral angle ϕ_i (black) and the pseudo-dihedral angles ν_i (orange), ξ_i (red), and μ_i (light gray) are identified as planar angles and obey the angular relationship: $\phi_i = \nu_i + \xi_i + \mu_i$; (e) Planar approach of image (a) structure concerning $\nu_i = 175°$ with the angular relationship described by $\phi_i = \nu_i + \xi_i + \mu_i$; (f) Analogous case of image (e), though in this case $\nu_i = -175°$ and the angular relationship is expressed by $\phi_i = \nu_i + \xi_i + \mu_i + 360°$.

rotation axis defined by atoms N^i and C^i_α to the z-axis of the Cartesian coordinate system [7]. In this case, the angular information required to rotate any point around the z-axis is the same as needed to rotate a point of the plane xy around its origin [7].

The relationship between the dihedral and pseudo-dihedral angles changes depending on the values of the pseudo-dihedral angles involved. Any relationship described from those angles can be considered a composition of rotations in the plane. Indeed, as $\mathbb{R}^2 \cong \mathbb{C}(\mathbb{R})$ [12], we assume without loss of generality that $C_\alpha = 0$ of $\mathbb{C}$ and the atoms C^{i-1}, C^i, H^i_α, and H^i_N are points of $\mathbb{C}$ in a unitary circle. Then, the following rotations in $\mathbb{C}$ allow the definition of the relative atomic positions:

$$C^i = e^{\mathbf{i}\phi_i} C^{i-1},\ C^i = e^{\mathbf{i}\xi_i} H^i_\alpha,\ H^i_\alpha = e^{\mathbf{i}\mu_i} H^i_N,\ \text{and}\ H^i_N = e^{\mathbf{i}\nu_i} C^{i-1}, \tag{3}$$

where $\mathbf{i}$ is the imaginary unity. From the rotations of (3), we can write:

$$\begin{aligned} &e^{\mathbf{i}\phi_i} C^{i-1} = e^{\mathbf{i}\xi_i} H^i_\alpha = e^{\mathbf{i}\xi_i} e^{\mathbf{i}\mu_i} H^i_N = e^{\mathbf{i}\xi_i} e^{\mathbf{i}\mu_i} e^{\mathbf{i}\nu_i} C^{i-1} = e^{\mathbf{i}(\xi_i+\mu_i+\nu_i)} C^{i-1} \Leftrightarrow \\ &\left(e^{\mathbf{i}\phi_i} - e^{\mathbf{i}(\xi_i+\mu_i+\nu_i)}\right) C^{i-1} = 0 \Leftrightarrow e^{\mathbf{i}\phi_i} = e^{\mathbf{i}(\xi_i+\mu_i+\nu_i)}. \end{aligned} \tag{4}$$

The solution for the complex number equation presented in (4) is given by

$$\phi_i = \nu_i + \xi_i + \mu_i + m \times 360^\circ, \tag{5}$$

such that $m \in \mathbb{Z}$. As all angles from (5) lie in the interval $(-180^\circ, 180^\circ]$, only $m \in \{-1, 0, 1\}$ must be considered in this solution.

A similar reasoning can be applied to describe the general case solution, which has pseudo-dihedral angles defined in atoms from the residues R_j, R_i and R_{i+1}, providing the equation (5):

$$\phi_i = \nu^{\kappa}_{ji} + \xi^{\rho}_i + \mu^{\kappa\rho}_{ji} + m \times 360^\circ, \text{ such that } m \in \{-1, 0, 1\}. \tag{6}$$

For a unique characterization of the result presented in (6), we must specify which value of m has to be considered in each circumstance. Theorem 1 provides a complete analysis.

Theorem 1. *Let R_j and R_i be amino acid residues of a protein, indexed by their positions in the primary sequence; ϕ_i, ν^{κ}_{ji}, ξ^{ρ}_i, and $\mu^{\kappa\rho}_{ji}$ be the dihedral and the three pseudo-dihedral angles defined in (1) and (2), respectively. The dihedral angle $\phi_i \in (-180^\circ,\ 180^\circ]$ can be written in the function of the other three pseudo-dihedral angles by $\phi_i = f_{m_\phi}\left(\Phi^{\kappa\rho}_{ji} + \mu^{\kappa\rho}_{ji}\right)$, where $\Phi^{\kappa\rho}_{ji} := \nu^{\kappa}_{ji} + \xi^{\rho}_i$,*

$$m_\phi := \begin{cases} 1 & \text{if } -180^\circ < \nu^{\kappa}_{ji} \leq -\xi^{\rho}_i, \\ -1 & \text{if } -\xi^{\rho}_i < \nu^{\kappa}_{ji} \leq 180^\circ, \end{cases} \quad \text{and}$$

$$f_m(\tau) := \begin{cases} \tau & \text{if } |\tau| < 180^\circ, \\ \tau + m \times 360^\circ & \text{if } |\tau| > 180^\circ, \\ 180^\circ & \text{if } |\tau| = 180^\circ. \end{cases} \tag{7}$$

Proof. As the pseudo-dihedral angles ν^{κ}_{ji} and $\mu^{\kappa\rho}_{ji}$ can assume any value in the interval $(-180^\circ, 180^\circ]$, to analyze all possibilities for these angles, conveniently, we consider the intervals: ⓘ : $-180^\circ < \nu^{\kappa}_{ji} \leq -\xi^{\rho}_i$ and ⓘⓘ : $-\xi^{\rho}_i < \nu^{\kappa}_{ji} \leq 180^\circ$; ① : $-180^\circ < \mu^{\kappa\rho}_{ji} \leq 0^\circ$ and ② : $0^\circ < \mu^{\kappa\rho}_{ji} \leq 180^\circ$. As it is mentioned in the examples, $-180^\circ < \xi^{\rho}_i < 0^\circ$; then:

$$ⓘ + ① \Rightarrow -360^\circ < \nu^{\kappa}_{ji} + \mu^{\kappa\rho}_{ji} \leq -\xi^{\rho}_i \Leftrightarrow \begin{cases} -360^\circ + \xi^{\rho}_i < \Phi^{\kappa\rho}_{ji} + \mu^{\kappa\rho}_{ji} \leq -180^\circ, \\ -180^\circ < \Phi^{\kappa\rho}_{ji} + \mu^{\kappa\rho}_{ji} \leq 0^\circ. \end{cases}$$

$$ⓘ + ② \Rightarrow \begin{cases} -180^\circ + \xi^{\rho}_i < \Phi^{\kappa\rho}_{ji} + \mu^{\kappa\rho}_{ji} \leq -180^\circ, \\ -180^\circ < \Phi^{\kappa\rho}_{ji} + \mu^{\kappa\rho}_{ji} \leq 180^\circ. \end{cases} \tag{8}$$

So, for case ⓘ, we remark:

$$\begin{cases} -360^\circ + \xi^{\rho}_i < \Phi^{\kappa\rho}_{ji} + \mu^{\kappa\rho}_{ji} < -180^\circ \\ -180^\circ \leq \Phi^{\kappa\rho}_{ji} + \mu^{\kappa\rho}_{ji} \leq 180^\circ \end{cases} \Leftrightarrow \begin{cases} \xi^{\rho}_i < \Phi^{\kappa\rho}_{ji} + \mu^{\kappa\rho}_{ji} + 360^\circ < 180^\circ \\ -180^\circ \leq \Phi^{\kappa\rho}_{ji} + \mu^{\kappa\rho}_{ji} \leq 180^\circ \end{cases} \tag{9}$$

Observing the result from (9) in (6), we can say:

$$\begin{cases} \phi_i = \Phi_{ji}^{\kappa\rho} + \mu_{ji}^{\kappa\rho} + 360^\circ & \text{if} \quad \Phi_{ji}^{\kappa\rho} + \mu_{ji}^{\kappa\rho} < -180^\circ, \\ \phi_i = \Phi_{ji}^{\kappa\rho} + \mu_{ji}^{\kappa\rho} & \text{if} \quad \left|\Phi_{ji}^{\kappa\rho} + \mu_{ji}^{\kappa\rho}\right| \leq 180^\circ. \end{cases} \tag{10}$$

With similar arguments from (8), for case (ii), we can write:

$$\begin{cases} \phi_i = \Phi_{ji}^{\kappa\rho} + \mu_{ji}^{\kappa\rho} & \text{if} \quad \left|\Phi_{ji}^{\kappa\rho} + \mu_{ji}^{\kappa\rho}\right| \leq 180^\circ, \\ \phi_i = \Phi_{ji}^{\kappa\rho} + \mu_{ji}^{\kappa\rho} - 360^\circ & \text{if} \quad \Phi_{ji}^{\kappa\rho} + \mu_{ji}^{\kappa\rho} > 180^\circ. \end{cases} \tag{11}$$

The results from (10) and (11) can be resumed by $\phi_i = f_{m_\phi}\left(\Phi_{ji}^{\kappa\rho} + \mu_{ji}^{\kappa\rho}\right)$, where f_m and m_ϕ are defined as the theorem presented them.

To determine the relationship among the angles ψ_i, υ_{ji}^{κ}, ζ_i^{ϱ}, and $\eta_{ji}^{\kappa\varrho}$, we can employ an identical strategy to the one presented to derive (6). As in the previous case, this result is given in Theorem 2, which can be proved similarly to Theorem 1.

Theorem 2. *Let R_j, R_i, and R_{i+1} be the amino acid residues of a protein, indexed by their positions in the primary sequence; ψ_i the dihedral angle defined in (1); υ_{ji}^{κ}, ζ_i^{ϱ}, and $\eta_{ji}^{\kappa\varrho}$ the pseudo-dihedral angles defined in (2). The dihedral angle $\psi_i \in (-180^\circ,\ 180^\circ]$ can be written in the function of the other three pseudo-dihedral by $\psi_i = f_{m_\psi}\left(\Psi_{ji}^{\kappa\varrho} + \eta_{ji}^{\kappa\varrho}\right)$ with, $\Psi_{ji}^{\kappa\varrho} := \upsilon_{ji}^{\kappa} + \zeta_i^{\varrho}$, f given by (7), and* $m_\psi := \begin{cases} 1 \ \text{if} -180^\circ < \upsilon_{ji}^{\kappa} \leq -\zeta_i^{\varrho}, \\ -1 \ \text{if} \quad -\zeta_i^{\varrho} < \upsilon_{ji}^{\kappa} \leq 180^\circ. \end{cases}$

In the next section we experimentally provide the numerical expressions proved by the theorems 1 and 2. Our experiments yield the association of the dihedral angles ϕ and ψ with the pseudo-dihedral angles μ and η, respectively, defined in two consecutive amino acid residues of a protein primary sequence. The results propose an estimation for the angular constants $\Phi_{ii}^{\varrho\rho}$ and $\Psi_{ii}^{\rho\varrho}$, with $\rho \in \{\alpha,\ \alpha_2\}$ and $\varrho \in \{N,\ \delta_3\}$.

3 Numerical experiments

A dataset of 226 protein structures was extracted from the list of NMR structures related to the training of the neural network TALOS-N [11], by picking up the first conformer of each structure, as explained in [3].

On the protein structures database, the angles ϕ, ψ, μ, and η are calculated using the python library MDAnalysis [2]. The amino acid residues are sorted into the following types: Glycines, Prolines, and Others. A linear regression is used to determine numerical slopes and intercepts of lines. For each case, at most two lines are observed. Fig. 2 shows the results of the plot $\mu \times \phi$; the regression parameters for this case are presented in Table 1. The numerical calculation of

$\eta \times \psi$ is given in Table 2. These numerical results allowed us to determine errors on the slopes and intercepts of the linear relationships presented in the theorems.

The distribution plots of the angles calculated on the database of protein structures are plotted (Fig. 3) using couples of dihedral backbone angles: ϕ/ψ (corresponding to the classical view of Ramachandran plots), μ/η, ϕ/η, and μ/ψ. Depending on the choice of the angle variable, the main secondary structure regions (α-Helix, β-Strand, and Loop) are displaced. For each secondary structure type, there is a combination of angles for which this region is connected in the modified Ramachandran map. This connectedness can simplify the application of the iBP algorithm, as the discontinuity due to the periodicity of angle values disappear for the considered secondary structure region.

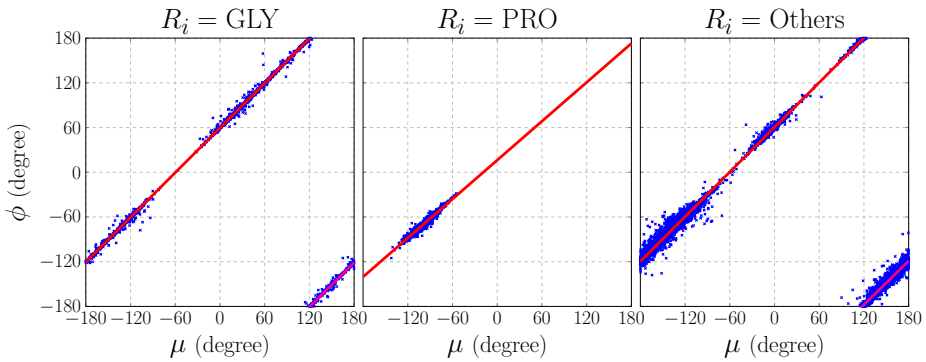

Fig. 2. Plots of $\phi \times \mu$ calculated on the protein database. The data are drawn in blue markers, and its linear regression by continuous lines in red and magenta. In the label of angle names, the first name denotes the x-axis label, and the second one the y-axis label.

Table 1. Linear Regression Parameters (L.R.P.), slope and intercept values, of the plot $\phi \times \mu$ regarding the equations $\phi_1(\mu) = a_1\mu + a_0$, $\phi_2(\mu) = b_1\mu + b_0$ analyzed on the protein data set.

L.R.P.	GLY	PRO	Others
a_1	1.0003 ± 0.0015	0.8739 ± 0.0137	0.9974 ± 0.0010
a_0	59.4967 ± 0.1477	16.2654 ± 1.3211	60.3836 ± 0.1375
b_1	0.9937 ± 0.0186	—	0.9767 ± 0.0060
b_0	-299.4858 ± 2.7960	—	-295.3706 ± 0.9490

4 Conclusions

The backbone dihedral angles ϕ and ψ were proposed in the 1950s to describe the curvilinear geometry of the protein backbone in the context of the newly developed X-ray crystallography approach for which the hydrogen positions were not visible in protein structures. Among the three main secondary structure

Table 2. Linear Regression Parameters (L.R.P.), slope and intercept values, of the plot $\psi \times \eta$ regarding the equations $\psi_1(\eta) = a_1\eta + a_0,\ \psi_2(\eta) = b_1\eta + b_0$, analyzed on the protein data set.

L.R.P.	R_i \ R_{i+1}	*cis* PRO	*trans* PRO	Others
a_1	GLY	—	0.9900 ± 0.0189	0.9992 ± 0.0013
a_0		—	139.2018 ± 0.8024	120.4346 ± 0.1393
b_1		—	0.9886 ± 0.0170	0.9999 ± 0.0042
b_0		—	-219.8191 ± 1.6198	-239.6703 ± 0.4781
a_1	Others	0.9163 ± 0.0805	1.0011 ± 0.0063	1.0004 ± 0.0003
a_0		81.5530 ± 5.2555	137.6785 ± 0.2224	119.3149 ± 0.0389
b_1		—	0.9896 ± 0.0187	0.9981 ± 0.0026
b_0		—	-221.6108 ± 2.9543	-240.2788 ± 0.3526

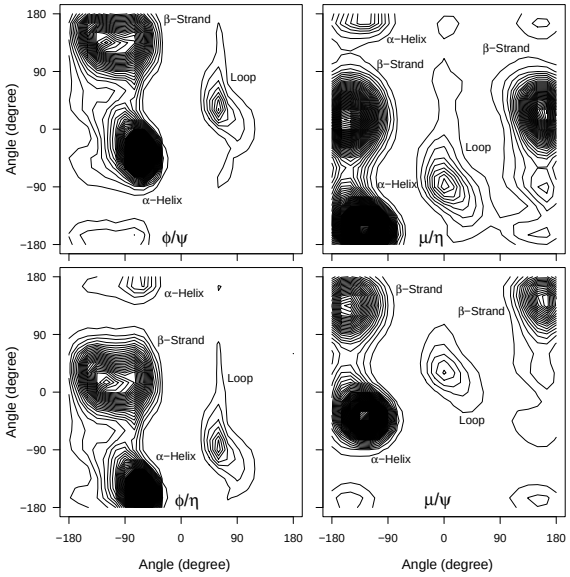

Fig. 3. Distribution of ϕ/ψ (upper left panel), μ/η (upper right panel), ϕ/η (lower left panel), and μ/ψ (lower right panel) angles. The first angles are plotted along the horizontal axes and the second along the vertical axes. The labels α-Helix, β-Strand, and Loop allow us to follow the displacements of the main secondary structures region on the Ramachandran plot according to the change of variables in angles.

regions, the β-Strand spread on regions in which ψ values display discontinuities jumping from $180°$ to $-180°$.

Extending the dihedral relationships to angles also involving hydrogen atoms, we proposed here new angles μ and η to describe the curvilinear geometry of the backbone angles. We proved precise relationships between ϕ and μ, and ψ and η. Analyzing the database of protein structures presented above, we obtained

numerical values and errors for slopes and intercepts describing the relationships between the angles ϕ, ψ, μ, and η. Combining new and old angles, the discontinuities present in the classical Ramachandran map can be suppressed.

During an iBP calculation, depending on the considered region of the map, the branching can be performed on-the-fly on dihedral angle combinations avoiding discontinuities. A similar approach could be derived, including long-range pseudo-dihedral angles involving atoms located in residues located far apart in the primary protein sequence, and would provide a new point of view on the description of protein structure. Indeed, most of the long-range descriptors are nowadays inter-atomic distances, and an angular perspective could bring new insights into protein geometry.

Acknowledgements CNRS, Lorraine University and ANR PRCI multiBioStruct (ANR-19-CE45-0019) are acknowledged for funding. Wagner Da Rocah thanks the ANR PRCI multiBioStruct (ANR-19-CE45-0019) project for postdoctoral support.

CNRS, Lorraine University, and ANR PRCI "Multi-scale and multi-resolution bio-molecular structure determination by geometric approaches - multiBioStruct" (ANR-19-CE45-0019) are acknowledged for funding. Wagner Da Rocha thanks the ANR PRCI multiBioStruct (ANR-19-CE45-0019) project for postdoctoral support.

References

1. Engh, R., Huber, R.: Accurate bond and angle parameters for X-ray protein structure refinement. Acta Crystallogr A **47**, 392–400 (1991)
2. Gowers, R., Linke, M., Barnoud, J., Reddy, T., Melo, M., Seyler, S., Dotson, D., Domanski, J., Buchoux, S., Kenney, I., Beckstein, O.: MDAnalysis: A Python package for the rapid analysis of molecular dynamics simulations. Proceedings of the 15th Python in Science Conference, Austin, TX, 2016 **32**, 102–109 (2016)
3. Khalife, S., Malliavin, T., Liberti, L.: Secondary structure assignment of proteins in the absence of sequence information. Bioinform Adv **1**, vbab038 (2021)
4. Lavor, C., Liberti, L., Mucherino, A.: The interval Branch-and-Prune algorithm for the discretizable molecular distance geometry problem with inexact distances. J Glob Optim **56**, 855–871 (2013)
5. Macari, G., Toti, D., Polticelli, F.: Computational methods and tools for binding site recognition between proteins and small molecules: from classical geometrical approaches to modern machine learning strategies. J Comput Aided Mol Des **33**, 887–903 (2019)
6. Malliavin, T.E., Mucherino, A., Lavor, C., Liberti, L.: Systematic Exploration of Protein Conformational Space Using a Distance Geometry Approach. J Chem Inf Model **59**, 4486–4503 (2019)
7. Marsh, D.: Applied Geometry for Computer Graphics and CAD. 2nd edn. Springer, London (2005)
8. Nelson, D.L. and Cox, M.M.: Lehninger Principles of Biochemistry: International Edition. W.H.Freeman & Co Ltd (2021)

9. Pan, X., Thompson, M.C., Zhang, Y., Liu, L., Fraser, J.S., Kelly, M.J.S., Kortemme, T.: Expanding the space of protein geometries by computational design of de novo fold families. Science **369**, 1132–1136 (2020)
10. Ramachandran, G., Ramakrishnan, C., Sasisekharan, V.: Stereochemistry of polypeptide chain configurations. Journal of Molecular Biology **7**, 95–99 (1963)
11. Shen, Y., Bax, A.: Protein structural information derived from NMR chemical shift with the neural network program TALOS-N. Methods Mol Biol **1260**, 17–32 (2015)
12. Suetin, P.K. and Kostrikin, A.I. and Manin, Y.I.: Linear Algebra and Geometry. Taylor & Francis (1997)
13. Zhao, J., Cao, Y., Zhang, L.: Exploring the computational methods for protein-ligand binding site prediction. Comput Struct Biotechnol J **18**, 417–426 (2020)